Emergent interactions due to resource competition in CRISPR-mediated genetic activation circuits*

Krishna Manoj[1] and Domitilla Del Vecchio[1]

Abstract— **CRISPR-mediated gene regulation has gained considerable attention due to its scalability, allowing to create increasingly large genetic circuits. Unintended interactions due to competition for the dCas9 resource among different small guide RNAs have been characterized extensively for CRISPR-mediated repression (CRISPRi). Such an analysis is to a large extent missing for CRISPR-mediated activation (CRISPRa). In this paper, we model CRISPRa considering two required shared resources (dCas9 and an activator protein), and identify the interaction graphs that emerge through resource competition. The presence of two shared resources among multiple scaffold RNAs (scRNA) is responsible for two main phenomena. First, we mathematically prove the existence of a "self-sequestration" effect, wherein an scRNA represses its own target gene instead of activating it, thereby negating the CRISPRa function. Second, we demonstrate that unwanted repression of non-target genes is substantially stronger when compared to a scenario with a single resource. These results indicate that new control approaches to concurrently regulate multiple resources will be useful for mitigating the undesirable effects of resource competition in CRISPRa.**

I. INTRODUCTION

Research on competition for shared resources has spanned to multiple domains of science. These domains include competition for food between primates [1], minerals between countries [2], environmental resources (light and water) in a forest [3], and breeding mates between rodents [4]. Beside such large scale systems, competition for shared resources can also occur at a cellular level. Examples include competition for ribosomes between various genes [5] or for shared protein resources (dCas9 for instance) during CRISPR-mediated gene regulation. In such cases, competition results in unintended coupling between genes through the shared resources, which leads to changes in the emergent behavior of a genetic circuit [6], [7], [8], [9].

CRISPR-mediated gene regulation has been widely used as a tool for transcriptional regulation due to its specificity and scalability. CRISPR-mediated repression (CRISPRi) and activation (CRISPRa) have been implemented in various systems by combining a dCas9 protein with a target specific gRNA or scRNA [10], [11]. Studies so far on competition in CRISPR-mediated gene regulation have considered dCas9 or modified dCas9 as the unique shared resource among multiple gRNAs or scRNAs. Recent experimental and theoretical studies on CRISPRi-based gene regulation have reported significant effects of competition on regulatory efficacy, and

dCas9 regulators have appeared to mitigate this problem [8], [7], [9].

There are two different major modalities for CRISPR-based gene activation. In the first modality, an activation domain is fused directly with the dCas9 protein to form an activator complex, such as dCas9-ω, dCas9-VP64, dCas9-p65AD, dCas9-RpoZ, dCas9-AsiA (Fig. 1a,c) [12]. In the second modality, an activator protein is a separate resource that binds with the scaffold RNA (scRNA), which, in turn, binds to dCas9 producing the sequence-specific activator complex that activates gene expression (Fig. 1b,d). Once the scRNA binds to the target promoter sequence, the activator protein recruits RNA polymerase to initiate transcription. Therefore, in this second modality, we have two resources: the dCas9 protein and the activator protein. The effect of competition for dCas9 is theoretically predicted to be negligible in the first modality of CRISPRa when compared to CRISPRi [13]. However, the effects of competition in the presence of two shared resources, as in the second modality of CRISPRa, is yet to be explored.

In this paper, we compare the two different modalities of CRISPRa: having a single shared resource (modality-1) and two shared resources (modality-2). In particular, the presence of two shared resources induces various combinations in which the sequence of bindings among the molecular players can occur, and thereby different chemical reaction routes for the activation of the output protein by an scRNA (compare Fig. 1c to Fig. 1d). We analyze the ordinary differential equation (ODE) models corresponding to the different routes and determine the emergent regulatory function, which includes both the intended regulation and the unintended one due to competition for resources. Subsequently, we mathematically study the derivative of the regulatory function to determine the sign of the unintended and emergent interactions. Further, we compare the extent of the unintended interaction obtained in modality-2 to that of modality-1 via simulations. Specifically, during modality-2, we observe a non-monotonic on-target emergent regulatory function, which is absent in modality-1. Furthermore, the extent of unintended interactions is substantially larger in modality-2, when compared to modality-1.

The outline of the paper is as follows: Section II introduces the reactions and the modeling framework of the system along with the regulatory and unintended interactions observed in modality-1. Section III performs a similar analysis of the emergent regulatory and unintended interactions on modality-2. In Section IV, we conclude the study and provide insights on possible future advancements and developments

[1]K. Manoj and D. Del Vecchio are with the Department of Mechanical Engineering, MIT, Cambridge, MA 02139, USA. Emails: kmanoj@mit.edu (K. Manoj), and ddv@mit.edu (D. Del Vecchio)
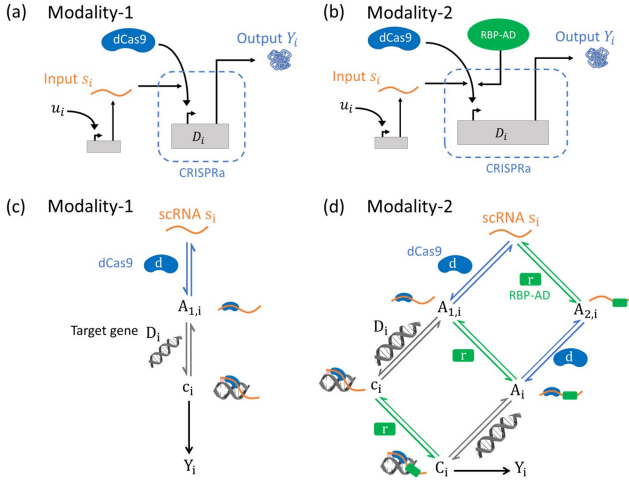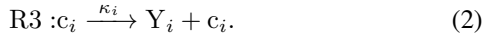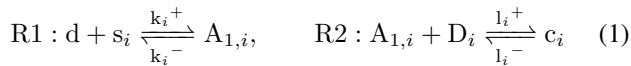
Fig. 1. CRISPRa-based gene regulation. (a-b) Genetic circuit diagrams corresponding to modality-1 (a) and modality-2 (b), in which scRNA (s_i) is the input to the CRISPRa module and the expressed protein (Y_i) is the output. In general, an scRNA itself can be an output, which, in turn, becomes an input to another CRISPRa module. RBP-AD represents the activator protein (RNA binding protein and activator domain unit), which is required for gene activation. (c,d) Chemical reaction diagrams corresponding to modality-1 (c) and modality-2. (d) Double-sided arrows represent reversible binding reactions. One-sided arrows represent the process of gene expression.

in the field.

II. CRISPRa MODALITY-1: SINGLE SHARED RESOURCE

In modality-1, we consider a pool of dCas9 or modified dCas9 (such as dCas9-ω, dCas9-VP64, dCas9-VP16, dCas9-YPet) as the single resource shared among sequence specific scRNAs or gRNAs. As shown in Fig. 1(c), the protein dCas9 binds with an scRNA (s_i, where $i \in [1, 2, 3, .., N]$, unless otherwise specified) to form a CRISPR activator complex, $A_{1,i}$. This complex acts as a transcription factor that activates the target gene, D_i, by forming the transcriptionally active complex, c_i, that results in transcription and translation to produce the output protein, Y_i. The route from scRNA to the output protein Y_i has a sequential structure (Fig. 1c). The chemical reactions corresponding to the reaction diagram of Fig. 1(c) can be written as:

$$\text{R1}: d + s_i \underset{k_i^-}{\overset{k_i^+}{\rightleftharpoons}} A_{1,i}, \qquad \text{R2}: A_{1,i} + D_i \underset{l_i^-}{\overset{l_i^+}{\rightleftharpoons}} c_i \quad (1)$$

$$\text{R3}: c_i \overset{\kappa_i}{\longrightarrow} Y_i + c_i. \quad (2)$$

The corresponding reaction rate equations can be obtained using mass action kinetics as [14]:

$$
\begin{aligned}
\dot{s}_i &= u_i + k_i^- A_{1,i} - k_i^+ d\, s_i - \delta s_i \\
\dot{A}_{1,i} &= k_i^+ d\, s_i - k_i^- A_{1,i} + l_i^- c_i - l_i^+ A_{1,i} D_i \\
\dot{c}_i &= l_i^+ A_{1,i} D_i - l_i^- c_i \\
\dot{Y}_i &= \kappa_i c_i - \gamma Y_i,
\end{aligned}
\quad (3)
$$

where, δ and γ are the corresponding decay rate constants of scRNAs and proteins. The decay rate constants of the intermediate complexes due to dilution and degradation are neglected when compared to the reverse binding reaction rate

constants (k_i^- and l_i^-, which are much larger in general [14]). In this system, the total concentration of dCas9 and DNA are conserved:

$$d_t = d + \Sigma_{i=1}^{N} A_{1,i} + \Sigma_{i=1}^{N} c_i \quad (4)$$

$$D_{it} = D_i + c_i, \quad (5)$$

where d_t and D_{it} are the total concentrations of dCas9 and target gene D_i, respectively. Since, the binding reactions in (1) are faster than production and decay of RNA and proteins [14], $A_{1,i}$ and c_i can be approximated at the quasi-steady state:

$$A_{1,i} = \frac{d s_i}{K_k} \quad \text{and} \quad c_i = \frac{d s_i D_i}{K_k K_l}, \quad (6)$$

where $K_l = l_i^-/l_i^+$ and $K_k = k_i^-/k_i^+$. Note, in this study, if x_i^+ is the rate constant of the forward reaction and x_i^- is the rate constant of the reverse reaction, then $K_x = x_i^-/x_i^+$. Further, substituting (6) in (5), we obtain the concentration for free target DNA, D_i, as follows:

$$D_i = \frac{D_{it}}{1 + \frac{d s_i}{K_k K_l}}. \quad (7)$$

Substituting (6) and (7) in (3) and (4), we obtain the final set of ODEs for the reduced system describing the dynamics of CRISPR mediated activation:

$$
\begin{aligned}
\dot{s}_i &= u_i - \delta s_i \\
\dot{Y}_i &= \underbrace{\frac{\kappa D_{it} d s_i}{d s_i + K_k K_l}}_{F_i(s_i, d), \text{ effective regulatory function}} - \gamma Y_i,
\end{aligned}
$$

$$G(s_i, d) := d + \Sigma_{i=1}^{N} \frac{d s_i}{K_k} + \Sigma_{i=1}^{N} \frac{D_{it} d s_i}{d s_i + K_k K_l} - d_t = 0. \quad (8)$$

The effect of sharing dCas9 manifests in the dynamics of Y_i through d, which depends on the concentration of other regulators, s_j, with $j \neq i$. This, in turn, gives rise to unintended interactions along with the intended regulatory interactions in the system, which can be captured by the following derivative:

$$
\frac{dF_i}{ds_j} = \overbrace{\underbrace{\frac{\partial F_i}{\partial s_j}}_{\text{positive or zero}}}^{\text{regulatory interaction}} + \overbrace{\underbrace{\frac{\partial F_i}{\partial d} \frac{dd}{ds_j}}_{\text{negative}}}^{\text{unintended interaction}}
$$

$$
= \begin{cases} \alpha(1 - \beta), & \text{if } i = j \\ -\alpha\beta, & \text{if } i \neq j, \end{cases}
$$

where,

$$\alpha = \frac{\kappa D_{it} d K_k K_l}{(d s_i + K_k K_k)^2}$$

$$\beta = \frac{\frac{s_i}{K_k} + \frac{D_{jt} s_i K_k K_l}{(d s_j + K_k K_l)^2}}{1 + \Sigma_{k=1}^{N} \frac{s_k}{K_k} + \Sigma_{k=1}^{N} \frac{D_{kt} s_k K_k K_l}{(d s_k + K_k K_l)^2}} < 1,$$

implying that $dF_i/ds_j > 0$ for $i = j$ and $dF_i/ds_j < 0$ for $i \neq j$. These regulatory and unintended interactions are shown in Fig. 2(a).
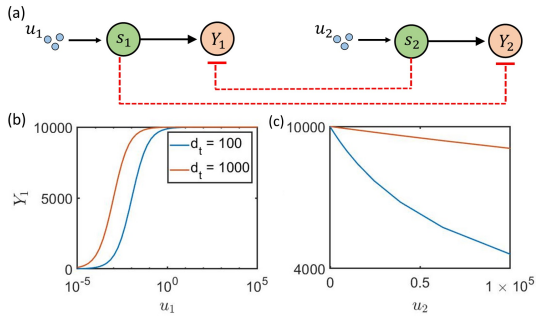
Fig. 2. Modality-1 of CRISPRa: effects of competition for a single shared resource. (a) Regulatory (black) and unintended (dashed red) interactions between nodes during CRISPR mediated activation in two parallel CRISPRa modules showing the effects of competition for shared resources. (b) Activation observed as u_1 is increased for different values of d_t. u_2 is kept constant at 0 nM. (c) Hidden repression observed in the production of Y_1 with increasing amounts of u_2. u_1 is kept constant at 10^2 nM. Other parameter values are $K_k = K_l = 0.1nM$, $D_{it} = 10nM$, $\gamma = 1hr^{-1}$, $\delta = 100hr^{-1}$ and, $\kappa = 1000hr^{-1}$.

Figure 2 (b-c) shows the effect of the unintended interactions on the steady state input-output characteristics of two parallel CRISPRa modules. The reduction of Y_1 as u_2 is increased occurs due to the hidden repression induced by competition for dCas9 between scRNAs. This effect diminishes when there are abundant resources in the system. Mathematically, when abundant resources are present in the system, (8) can be approximated as $d \approx d_t$, which gives us the reduced system of the form:

$$\dot{Y}_i = \underbrace{\frac{\kappa D_{it} d_t s_i}{d_t s_i + K_k K_l}}_{F_i(s_i)} - \gamma Y_i,$$

eliminating the indirect coupling between s_j and Y_i. However, there is a limit to the extent by which dCas9 can be increased due to its toxicity [9]. Therefore, increasing dCas9 concentration may not be a practically feasible approach to mitigate the effects of competition. Having characterized competition effects in modality-1, we perform a similar characterization for modality-2 in the upcoming section.

III. CRISPRa MODALITY-2: TWO SHARED RESOURCES

In modality-2, the reaction network consists of target specific scRNAs (s_i), their corresponding target genes (D_i), and two shared resources, dCas9 (d) and RBP-AD activator protein (r). As the scRNA functions as a backbone that binds with dCas9, recruits the RBP-AD unit, and recognizes the DNA target site, s_i will mediate the formation of the activator complex. Secondly, dCas9 protein is essential for binding to the DNA [15]. This leads to the set of all possible reactions as depicted in the reaction diagram of Fig. 1(d). We analyze the behaviors emerging from this "double diamond" reaction structure by viewing it as the combination of three different routes to gene activation (Scenarios 1-3 in Fig 3), described subsequently.

Route 1: During route 1, the scRNA (s_i) binds with the dCas9 protein (d) forming an intermediate $A_{1,i}$ complex, which recruits the RBP-AD unit forming the CRISPR
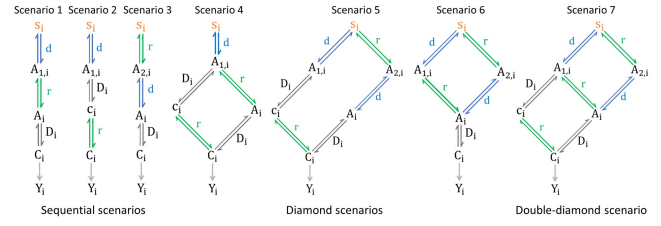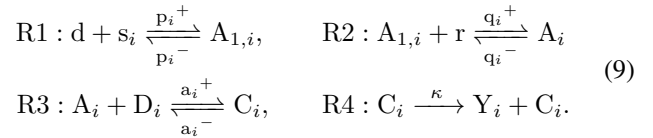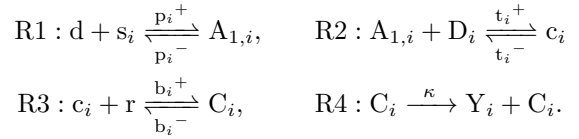

Fig. 3. Chemical reaction diagrams corresponding to different scenarios in modality-2. These include sequential scenarios (scenario 1-3), diamond scenarios (scenario 4-6) and double-diamond scenario (scenario 7).
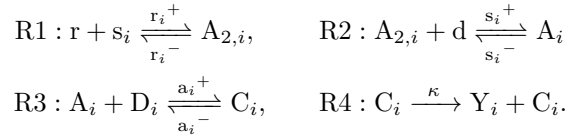
activator complex (A_i). The activator complex acts as a transcription factor, binds with the target gene to produce the transcriptionally active complex C_i, which produces the output protein Y_i. The chemical reactions are as follows:

$$R1 : d + s_i \underset{p_i^-}{\overset{p_i^+}{\rightleftharpoons}} A_{1,i}, \qquad R2 : A_{1,i} + r \underset{q_i^-}{\overset{q_i^+}{\rightleftharpoons}} A_i$$

$$R3 : A_i + D_i \underset{a_i^-}{\overset{a_i^+}{\rightleftharpoons}} C_i, \qquad R4 : C_i \overset{\kappa}{\longrightarrow} Y_i + C_i. \qquad (9)$$

Route 2: In this route, the $A_{1,i}$ complex formed by the binding between dCas9 and scRNA, binds with the target gene prior to the recruitment of the RBP-AD unit, forming a complex that we refer as c_i. c_i then recruits the RBP-AD unit to form complex C_i. The reactions are as follows:

$$R1 : d + s_i \underset{p_i^-}{\overset{p_i^+}{\rightleftharpoons}} A_{1,i}, \qquad R2 : A_{1,i} + D_i \underset{t_i^-}{\overset{t_i^+}{\rightleftharpoons}} c_i$$

$$R3 : c_i + r \underset{b_i^-}{\overset{b_i^+}{\rightleftharpoons}} C_i, \qquad R4 : C_i \overset{\kappa}{\longrightarrow} Y_i + C_i.$$

Route 3: In route 3, the formation of the activator unit takes a different path, where the scRNA binds with the RBP-AD unit prior to dCas9, forming the intermediate $A_{2,i}$ complex. This is followed by the binding reaction between $A_{2,i}$ and the dCas9 protein, forming the activator complex (A_i). The reactions are as follows:

$$R1 : r + s_i \underset{r_i^-}{\overset{r_i^+}{\rightleftharpoons}} A_{2,i}, \qquad R2 : A_{2,i} + d \underset{s_i^-}{\overset{s_i^+}{\rightleftharpoons}} A_i$$

$$R3 : A_i + D_i \underset{a_i^-}{\overset{a_i^+}{\rightleftharpoons}} C_i, \qquad R4 : C_i \overset{\kappa}{\longrightarrow} Y_i + C_i.$$

Having presented the three possible routes to gene activation in modality-2, we devise multiple possible scenarios in which the three routes can combine: the isolated (sequential), pair-combination (diamond network) and complete combination (double diamond network) scenarios (Fig. 3). In the following sections, we analyze the behavior of Y_i as a function of s_j for each type of scenario considered.

A. Sequential scenarios: Scenarios 1,2,3

Scenarios 1, 2, and 3 correspond to the individual appearance of routes 1, 2, and 3, respectively.

Scenario 1: From the reactions given in (9), we obtain the

reaction rate equations as:

$$\dot{Y}_i = \kappa C_i - \gamma Y_i$$
$$\dot{C}_i = a^+ A_i D_i - a^- C_i$$
$$\dot{A}_i = q^+ A_{1,i} r - q^- A_i - a^+ A_i D_i + a^- C_i \qquad (10)$$
$$\dot{A}_{1,i} = p^+ s_i d - p^- A_{1,i} - q^+ A_{1,i} r + q^- A_i$$
$$\dot{s}_i = u_i - \delta s_i - p^+ s_i d + p^- A_{1,i}.$$

Accounting for the time scale separation between the binding reactions and the protein and scRNA production and decay rates, we set the intermediate complexes to the quasi-steady state, and $K = K_a K_p K_q$ to obtain:

$$A_{1,i} = \frac{s_i d}{K_p}, \quad A_i = \frac{s_i d\ r}{K_q K_p} \quad \text{and} \quad C_i = \frac{D_i s_i d\ r}{K}.$$

Using the conservation of target gene ($D_{it} = D_i + C_i$), dCas9 ($d_t = d + \Sigma_i C_i + \Sigma_i A_i + \Sigma_i A_{1,i}$) and RBP-AD ($r_t = r + \Sigma_i C_i + \Sigma_i A_i$), we obtain:

$$D_i = \frac{D_{it} K}{K + s_i d\ r} \qquad (11)$$

$$d_t = d + \Sigma_{i=1}^N \left[1 + \frac{r}{K_q}\left(1 + \frac{D_i}{K_a}\right) \right] \frac{d s_i}{K_p} \qquad (12)$$

$$r_t = r + \Sigma_{i=1}^N \left(1 + \frac{D_i}{K_a}\right) \frac{r\ d\ s_i}{K_q K_p}. \qquad (13)$$

Therefore, system (10) reduces to

$$\dot{s}_i = u_i - \delta s_i \quad \text{and} \quad \dot{Y}_i = \kappa \underbrace{\frac{D_{it} s_i d\ r}{K + s_i d\ r}}_{F_i^1(s_i,d,r)} - \gamma Y_i. \qquad (14)$$

The effect of competition is manifested by the dependence of d and r in the expression of F_i^1 on s_j for $j \neq i$. This is made precise by the following claim.

Claim 1. *In the system given by (11) - (14), we have that:*

$$\frac{dF_i^1}{ds_j} \begin{cases} > 0, & \text{if } j = i \\ < 0, & \text{if } j \neq i. \end{cases}$$

Proof: Using the expression of F_i^1 given in (14) and the fact that r and d are functions of $s_1, ..., s_N$ by (12)-(13), we have:

$$\frac{dF_i^1}{ds_j} = \underbrace{\frac{\partial F_i^1}{\partial s_j}}_{\text{regulatory interactions}} + \underbrace{\frac{\partial F_i^1}{\partial d} \frac{dd}{ds_j} + \frac{\partial F_i^1}{\partial r} \frac{dr}{ds_j}}_{\text{unintended interactions}}. \qquad (15)$$

Calculating each term individually using (14), we obtain:

$$\frac{\partial F_i^1}{\partial s_j} = \begin{cases} \frac{\kappa K D_{it} d\ r}{(K + d\ r s_i)^2}, & \text{if } i = j \\ 0, & \text{if } i \neq j \end{cases},$$

$$\frac{\partial F_i^1}{\partial d} = \frac{\kappa K D_{it} s_i r}{(K + d\ r s_i)^2} \quad \text{and} \quad \frac{\partial F_i^1}{\partial r} = \frac{\kappa K D_{it} s_i d}{(K + d\ r s_i)^2}.$$

Applying differentiation with respect to s_i on the conservation laws for d and r given in (12) and (13), we obtain two
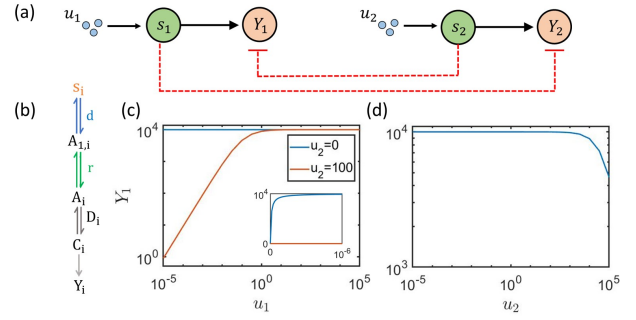

Fig. 4. Regulatory and unintended interactions for the sequential scenarios in modality-2. (a) Intended and hidden interactions between nodes of two parallel scRNA systems. (b) Scenario 1 is used as a representative example. (c) Input/output response for Y_1 with respect to its input u_1 in the absence ($u_2 = 0$ nM) and in the presence ($u_2 = 100$ nM) of competition for shared resources (dCas9 and RBP-AD) between two scRNAs. (d) Y_1 with respect to the amount of the competitor input u_2 for $u_1 = 100$ nM. Inset in (c) shows a zoomed in view with linear scales for the u_1 and Y_1 axes. Other parameters: $D_{1t} = D_{2t} = 10$ nM, $d_t = 100$ nM, $r_t = 1000$ nM, $\gamma = 1 \text{hr}^{-1}$, $\delta = 100 \text{hr}^{-1}$. and, $\kappa = 1000 \text{hr}^{-1}$, $x_i^+ = 10$ and $x_i^- = 1$, where $x \in \{a, p, q\}$.

linear equations with two variables dd/ds_i and dr/ds_i. Solving the set of linear equations we obtain:

$$\frac{dd}{ds_i} = \frac{-d}{\Phi K_p}\left[1 + \Sigma_i \frac{s_i d}{K_p K_q} + \Sigma_i \frac{D_{it} ds_i K}{(K + d\ rs_i)^2} \right.$$
$$\left. + \frac{r}{K_p K_q} + \frac{D_{it} r K}{(K + d\ rs_i)^2} \right] < 0,$$

$$\frac{dr}{ds_i} = -\frac{1}{\Phi}\left[\frac{rd}{K_p K_q} + \frac{D_{it} d\ r K}{(K + d\ rs_i)^2} \right] < 0,$$

$$\Phi = \left[1 + \Sigma_i \frac{s_i d}{K_p K_q} + \Sigma_i \frac{D_{it} ds_i K}{(K + d\ rs_i)^2} \right]\left(1 + \Sigma_i \frac{s_i}{K_p} \right)$$
$$+ \Sigma_i \frac{rs_i}{K_p K_q} + \Sigma_i \frac{D_{it} rs_i K}{(K + d\ rs_i)^2}.$$

Substituting the above expressions in (15), we derive:

$$\frac{dF_i^1}{ds_j} = \begin{cases} \tilde{\alpha}(1 - \tilde{\beta}) > 0, & \text{if } i = j \\ -\tilde{\alpha}\tilde{\beta} < 0, & \text{if } i \neq j \end{cases}$$

where

$$\tilde{\alpha} = \frac{\kappa D_{it} d\ r K}{(K + d\ rs_i)^2},$$

$$\tilde{\beta} = \frac{s_i}{K_p \Phi}\left[1 + \Sigma_{k=1}^N \frac{s_k d}{K_p K_q} + \Sigma_{k=1}^N \frac{D_{kt} ds_k K}{(K + d\ rs_k)^2} + \frac{r}{K_p K_q} \right.$$
$$\left. + \frac{D_{it} r K}{(K + d\ rs_i)^2} \right] + \frac{ds_i}{K_p K_q \Phi} + \frac{D_{it} ds_i K}{\Phi(K + d\ rs_i)^2} < 1.$$
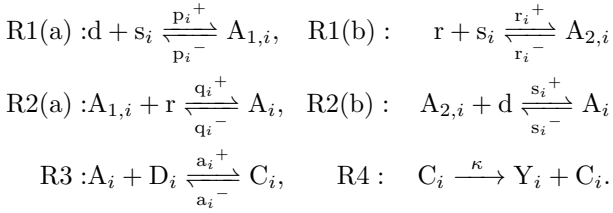
Figure 4(a) depicts the interactions characterized by Claim 1 in a graphical way. Also, numerical analysis of scenario 1 (Fig. 4b) confirms a monotonic increase in the output protein concentration Y_1 with increasing u_1 (Fig. 4c), and the unintended decrease in Y_1 with increasing levels of u_2 (Fig. 4d).

Scenarios 2 and 3: Although the analysis was performed in detail for scenario 1 alone, Claim 1 holds true for scenarios 2 and 3.

B. Diamond scenarios: Scenarios 4,5,6

Diamond scenarios refer to the combination of any two of the three routes and are depicted in Figure 3. Here, we provide the detailed analysis and claims for Scenario 6 only due to space limitations. However, the same claim will hold for Scenarios 4 and 5.

Scenario 6: The scRNA binds with either shared resources, dCas9 (R1(a)) or RBP-AD (R1(b)) to form the intermediate complex $A_{1,i}$ or $A_{2,i}$, respectively. These intermediate complexes bind with the remaining shared resource (R2) to form the activator complex A_i, which then binds with the target gene forming C_i and ultimately producing Y_i. This diamond scenario is given by the following set of reactions:

$$\text{R1(a)}: d + s_i \underset{p_i^-}{\overset{p_i^+}{\rightleftharpoons}} A_{1,i}, \quad \text{R1(b)}: \quad r + s_i \underset{r_i^-}{\overset{r_i^+}{\rightleftharpoons}} A_{2,i}$$

$$\text{R2(a)}: A_{1,i} + r \underset{q_i^-}{\overset{q_i^+}{\rightleftharpoons}} A_i, \quad \text{R2(b)}: \quad A_{2,i} + d \underset{s_i^-}{\overset{s_i^+}{\rightleftharpoons}} A_i$$

$$\text{R3}: A_i + D_i \underset{a_i^-}{\overset{a_i^+}{\rightleftharpoons}} C_i, \quad \text{R4}: \quad C_i \overset{\kappa}{\longrightarrow} Y_i + C_i.$$

From the above reactions, the reaction rate equations are:

$$
\begin{aligned}
\dot{Y}_i &= \kappa C_i - \gamma Y_i \\
\dot{C}_i &= a^+ A_i D_i - a^- C_i \\
\dot{A}_i &= q^+ A_{1,i} r + s^+ A_{2,i} d + a^- C_i - (q^- + s^- - a^+ D_i) A_i \\
\dot{A}_{1,i} &= p^+ s_i d - p^- A_{1,i} - q^+ A_{1,i} r + q^- A_i \\
\dot{A}_{2,i} &= r^+ r s_i + s^- A_i - r^- A_{2,i} - s^+ A_{2,i} d \\
\dot{s}_i &= u_i - p^+ s_i d + p^- A_{1,i} - r^+ r s_i + r^- A_{2,i} - \delta s_i.
\end{aligned}
\tag{16}
$$

Neglecting the decay rate constants of intermediate complexes and assuming them to be at the quasi steady state, we obtain the following expression:

$$A_i = \left[\frac{p_i^+ q_i^+ (r_i^- + s_i^+ d) + r_i^+ s_i^+ (p_i^- + q_i^+ r)}{p_i^- q_i^- (r_i^- + s_i^+ d) + r_i^- s_i^- (p_i^- + q_i^+ r)} \right] s_i d \, r. \tag{17}$$

Using (16) and (17), the conservation laws for the target gene ($D_{it} = D_i + C_i$), dCas9 ($d_t = d + \Sigma_i C_i + \Sigma_i A_i + \Sigma_i A_{1,i}$) and RBP-AD ($r_t = r + \Sigma_i C_i + \Sigma_i A_i + \Sigma_i A_{2,i}$) are simplified as:

$$D_i = \frac{D_{it}}{1 + \frac{A_i}{K_a}}$$

$$d_t = d + \Sigma_{i=1}^N \frac{A_i D_{it}}{K_a + A_i} + \Sigma_{i=1}^N A_i + \Sigma_{i=1}^N \frac{p_i^+ s_i d + q_i^- A_i}{p_i^- + q_i^+ r} \tag{18}$$

$$r_t = r + \Sigma_{i=1}^N \frac{A_i D_{it}}{K_a + A_i} + \Sigma_{i=1}^N A_i + \Sigma_{i=1}^N \frac{r_i^+ r s_i + s_i^- A_i}{r_i^- + s_i^+ d}. \tag{19}$$

The reaction rate equations can therefore be simplified as:

$$\dot{s}_i = u_i - \delta s_i$$

$$\dot{Y}_i = \kappa \underbrace{\frac{D_{it} A_i}{K_a + A_i}}_{F_i^6(s_i, d, r)} - \gamma Y_i. \tag{20}$$

Claim 2. *The system given by (18) - (20) with a single scRNA (N=1) exhibits self-sequestration, that is:*

$$\frac{\mathrm{d} F_i^6}{\mathrm{d} s_i} \begin{cases} > 0, & \text{for low } s_i \\ < 0, & \text{for high } s_i \end{cases}.$$

Proof: Using the reduced reaction rate equations in (20), we derive:

$$\frac{\mathrm{d} F_i^6}{\mathrm{d} s_i} = \frac{\kappa D_{it} K_a}{(K_a + A_i)^2} \frac{\mathrm{d} A_i}{\mathrm{d} s_i}. \tag{21}$$

Therefore, we move our focus, to derive an expression for $\mathrm{d}A_i/\mathrm{d}s_i$. For ease of calculating the derivatives, (18) and (19), can be equivalently written as follows:

$$
\begin{aligned}
X_i(s_i, r, d) :=& (r^+ s_i r + s^- A_i)(p^- + q^+ r + p^+ s_i) \\
& + \left[r_t - r - A_i \left(1 + \frac{D_{it}}{K_a + A_i} \right) \right] \left[s^+ A_i(q^- + \frac{D_{it}(p^- + q^+ r)}{K_a + A_i}) \right. \\
& \left. - r^-(p^- + q^+ r + p^+ s_i) - s^+(p^- + q^+ r)(d_t - A_i) \right] = 0
\end{aligned}
$$

$$
\begin{aligned}
Z_i(s_i, r, d) :=& (p^+ s_i d + q^- A_i)(r^- + s^+ d + r^+ s_i) \\
& + \left[d_t - d - A_i \left[1 + \frac{D_t}{K_a + A_i} \right] \right] \left[q^+ A_i(s^- + \frac{D_{it}(r^- + s^+ d)}{K_a + A_i}) \right. \\
& \left. - p^-(r^- + s^+ d + r^+ s_i) - q^+(r^- + s^+ d)(r_t - A_i) \right] = 0.
\end{aligned}
$$

Taking the derivative of (17) with respect to s_i, we obtain:

$$\frac{\mathrm{d} A_i}{\mathrm{d} s_i} = \frac{\partial A_i}{\partial s_i} + \frac{\partial A_i}{\partial r} \frac{\mathrm{d} r}{\mathrm{d} s_i} + \frac{\partial A_i}{\partial d} \frac{\mathrm{d} d}{\mathrm{d} s_i}.$$

Here, the terms $\frac{\partial A_i}{\partial s_i}$, $\frac{\partial A_i}{\partial r}$ and $\frac{\partial A_i}{\partial d}$ are calculated using (17) and are all non negative (zero or positive depending on s_i). The implicit function theorem is then applied on $X_i(s_i, r, d)$ and $Z_i(s_i, r, d)$ to obtain $\frac{\mathrm{d} r}{\mathrm{d} s_i}$ and $\frac{\mathrm{d} d}{\mathrm{d} s_i}$, which are strictly negative irrespective of s_i. Subsequently, we apply limits of s_i tending to zero and infinity, to examine the behavior of $\frac{\mathrm{d} A_i}{\mathrm{d} s_i}$, and obtain:

$$\lim_{s_i \to 0} \frac{\mathrm{d} A_i}{\mathrm{d} s_i} = \frac{\partial A_i}{\partial s_i} > 0$$

$$\lim_{s_i \to \infty} \frac{\mathrm{d} A_i}{\mathrm{d} s_i} = \underbrace{\frac{\partial A_i}{\partial r}}_{\text{positive}} \underbrace{\frac{\mathrm{d} r}{\mathrm{d} s_i}}_{\text{negative}} + \underbrace{\frac{\partial A_i}{\partial d}}_{\text{positive}} \underbrace{\frac{\mathrm{d} d}{\mathrm{d} s_i}}_{\text{negative}} < 0.$$

Hence, we can conclude that $\frac{\mathrm{d} A_i}{\mathrm{d} s_i}$ is positive for low s_i and negative for high s_i. From (21), we know that $\mathrm{d}F_i^6/\mathrm{d}s_i$ is a positive function of A_i multiplied with $\mathrm{d}A_i/\mathrm{d}s_i$, therefore it shows a similar qualitative behavior.

Claim 3. *For the system given by (18) - (20) we have that,*

$$\frac{\mathrm{d} F_i^6}{\mathrm{d} s_j} < 0, \quad \text{for } i \neq j.$$

Proof: Using a similar approach as in Claim 2, we derive:

$$\frac{\mathrm{d} F_i^6}{\mathrm{d} s_j} = \frac{\kappa D_{it} K_a}{(K_a + A_i)^2} \frac{\mathrm{d} A_i}{\mathrm{d} s_j}.$$

Taking the derivative of (17) with respect to s_j, we obtain:

$$\frac{\mathrm{d} A_i}{\mathrm{d} s_j} = \frac{\partial A_i}{\partial s_j} + \frac{\partial A_i}{\partial r} \frac{\mathrm{d} r}{\mathrm{d} s_j} + \frac{\partial A_i}{\partial d} \frac{\mathrm{d} d}{\mathrm{d} s_j}.$$
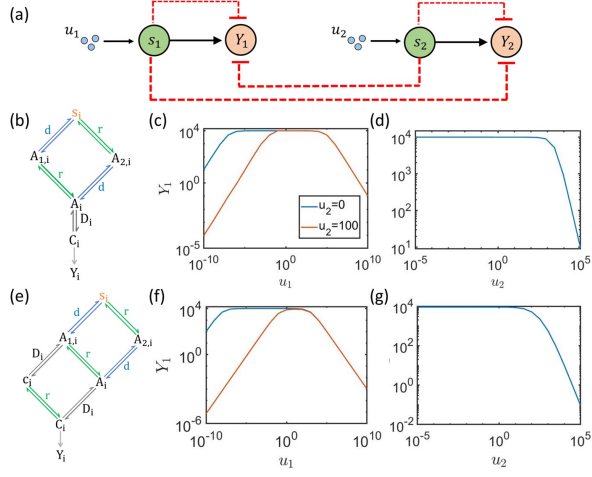
Fig. 5. Regulatory and unintended interactions for the single and double diamond scenarios in modality-2. (a) Intended (solid black) and hidden interactions (dashed red) between nodes of two parallel scRNA systems in diamond and double diamond scenarios. (b) single diamond scenario (scenario 6) used for the simulations in (c) and (d). (c) Input/output response for Y_1 with respect to its corresponding input u_1 in the absence ($u_2 = 0$ nM) and the presence ($u_2 = 100$ nM) of competition for shared resources (dCas9 and RBP-AD) between two scRNAs and (d) Y_1 with respect to the amount of the competitor input u_2 for $u_1 = 100$ nM. (e) Double diamond scenario (scenario 7) used for the simulations in (f) and (g). (f)-(g) same as in (c)-(d) but for (e) scenario 7. Other parameters: Same as Fig. 4 with $x \in \{a, b, p, q, r, s, t\}$.

Calculating these derivatives individually using (17) and the conservation laws in (18) and (19), we obtain:

$$\frac{\mathrm{d}A_i}{\mathrm{d}s_j} = \underbrace{\frac{\partial A_i}{\partial s_j}}_{Zero} + \underbrace{\frac{\partial A_i}{\partial r}}_{positive} \underbrace{\frac{\mathrm{d}r}{\mathrm{d}s_j}}_{negative} + \underbrace{\frac{\partial A_i}{\partial d}}_{positive} \underbrace{\frac{\mathrm{d}d}{\mathrm{d}s_j}}_{negative} \, .$$

Therefore, $\frac{\mathrm{d}A_i}{\mathrm{d}s_j} < 0$, implying that $\frac{\mathrm{d}F_i^6}{\mathrm{d}s_j} < 0$ for $i \neq j$.

Figure 5a shows the unintended interactions in red. Further, numerical analysis of scenario 6 (Fig. 5b) confirms the self-sequestration behaviour with a steady increase in the concentration of Y_1 for low values of u_1, as expected due to the regulatory effect, followed by a decline for high u_1 (Fig. 5c). Such a self sequestration in the absence of competition with other scRNAs occurs due to the diamond structure of the network and is not observed in the sequential scenarios or in modality-1.

The unintended competition for shared resources between the scRNAs and the intermediate complexes leads to self-sequestration. Specifically, an increase in the input u_1 increases s_1, which causes a decline in the concentration of free shared resources (d and r). The concentration of the intermediate complexes, $A_{1,i}$ and $A_{2,i}$, and of the activator complex A_i, therefore, increases. The limited amount of shared resources, causes a competition for the free dCas9 and RBP-AD molecules between s_i, and the intermediate complexes. At high concentrations of s_i, the production of the intermediate complexes are preferred over the production of A_i. Such a behavior leads to a decrease in the concentration of A_i for large u_i. The decline continues until A_i tends to zero and the concentration of the intermediate

complexes reaches a pinnacle after using up the shared resources completely. Therefore, the presence of the diamond structure results in the hoarding of the available resources by the intermediate complexes formed in the upper half of the diamond. This results in the reduction of available resources for the reactions in the downward half of the diamond, thereby causing a repression in the production of the output. Although the analytical proof is performed for $N = 1$, numerical simulations show that the bitonic behavior is observed for any value of N (Fig. 5c).
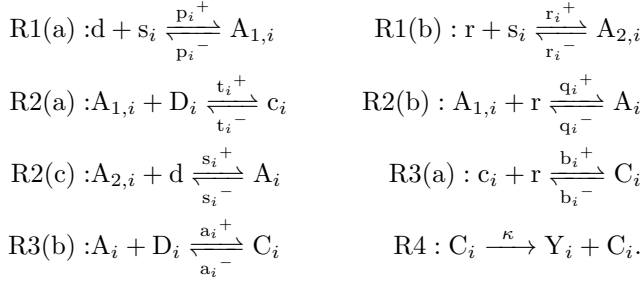
The addition of competition in the system leads to the occurrence of unintended off-target repression (Claim 3), which is confirmed numerically in Fig. 5d. By comparing the plots in Fig. 5(d) and Fig. 4(d), we can infer that the extent to which competition effects the production of the output protein is larger in Fig. 5(d) than in Fig. 4(d). This can be explained as follows. Increase in u_2 results in the competition for the shared resources, dCas9 and RBP-AD, between s_1, s_2 and the corresponding intermediate complexes in diamond scenarios, unlike the sequential scenario where the competition is between s_1 and s_2, alone. Such an increase in the number of competitors causes a much more significant reduction in the output protein concentration, Y_1, during diamond scenarios when compared to sequential scenarios. Hence, we observe that the effect of competition for resources occurs at significant levels in the diamond scenarios.

Although the above analytical and numerical analysis is based on scenario 6, similar qualitative behavior is observed and can be derived for scenarios 4 and 5. The extent of self-sequestration and competition depends on the total values of dCas9 and RBP-AD molecules in the system and may vary among the scenarios. In conclusion, comparing the results in modality-1 and the diamond scenario of modality-2, we observe the emergence of the self-sequestration behavior along with a significant effect of competition that emerges due to the diamond network structure.

C. Double diamond scenario: Scenario 7

During this scenario, we have the simultaneous occurrence of all three routes from scRNA to the output protein, forming a double diamond network structure (Fig. 5e). During this scenario, the scRNA can bind with dCas9 through the reaction R1(a) or to RBP-AD through R1(b) forming $A_{1,i}$ and $A_{2,i}$, respectively. In the subsequent reaction, the intermediate complex $A_{1,i}$ can bind either with the shared resource RBP-AD or the target gene producing A_i and c_i, respectively, through the reaction R2(a) and R2(b). The intermediate complex $A_{2,i}$ binds with RBP-AD forming A_i through reaction R2(c). In the following reaction, c_i recruits RBP-AD through R3(a) and A_i binds with the target gene through R3(b), forming the transcriptionally active complex C_i. Finally, C_i undergoes transcription and translation producing the output protein Y_i. The following are the chemical

reactions for the double diamond scenario:

$$\text{R1(a)}: d + s_i \underset{p_i^-}{\overset{p_i^+}{\rightleftharpoons}} A_{1,i} \qquad\qquad \text{R1(b)}: r + s_i \underset{r_i^-}{\overset{r_i^+}{\rightleftharpoons}} A_{2,i}$$

$$\text{R2(a)}: A_{1,i} + D_i \underset{t_i^-}{\overset{t_i^+}{\rightleftharpoons}} c_i \qquad \text{R2(b)}: A_{1,i} + r \underset{q_i^-}{\overset{q_i^+}{\rightleftharpoons}} A_i$$

$$\text{R2(c)}: A_{2,i} + d \underset{s_i^-}{\overset{s_i^+}{\rightleftharpoons}} A_i \qquad\quad \text{R3(a)}: c_i + r \underset{b_i^-}{\overset{b_i^+}{\rightleftharpoons}} C_i$$

$$\text{R3(b)}: A_i + D_i \underset{a_i^-}{\overset{a_i^+}{\rightleftharpoons}} C_i \qquad\quad \text{R4}: C_i \xrightarrow{\kappa} Y_i + C_i.$$

Using the above reactions, the reaction rate equations can be derived as:

$$\dot{Y}_i = \kappa C_i - \gamma Y_i$$
$$\dot{C}_i = a^+ A_i D_i + b^+ c_i r - (a^- + b^-)C_i$$
$$\dot{A}_i = q^+ A_{1,i} r + s^+ A_{2,i} d + a^- C_i - (q^- + s^- + a^+ D_i)A_i$$
$$\dot{A}_{2,i} = r^+ r s_i + s^- A_i - (r^- + s^+ d)A_{2,i}$$
$$\dot{A}_{1,i} = p^+ s_i d + q^- A_i + t^- c_i - (p^- + q^+ r + t^+ D_i)A_{1,i}$$
$$\dot{s}_i = u_i + p^- A_{1,i} + r^- A_{2,i} - p^+ s_i d - r^+ r s_i - \delta s_i.$$

The conservation laws for the two shared resources and the target gene can be obtained as: DNA: $D_{it} = D_i + C_i + c_i$, dCas9: $d_t = d + \Sigma_i C_i + \Sigma_i A_i + \Sigma_i c_i + \Sigma_i A_{1,i}$ and RBP-AD: $r_t = r + \Sigma_i C_i + \Sigma_i A_i + \Sigma_i A_{2,i}$. Numerically solving the above set of reaction rate equations along with the conservation laws, we obtain the steady state response as shown in Fig. 5(f,g). The behavior is similar to the single diamond scenario with the occurrence of self-sequestration in the absence and the presence of the competitor scRNA. Furthermore, a significant increase in the extent of unintended interaction causing a decrease in the output concentration when compared to sequential (Fig. 4d) and diamond (Fig. 5d) scenarios is observed for double-diamond scenarios (Fig. 5g).

IV. DISCUSSION AND CONCLUSIONS

Gene specificity of CRISPR mediated regulation led to utilizing CRISPRi and CRISPRa in multiplexing and genetic circuit design. However, increasing the complexity of circuits based on CRISPR gene regulation engenders hidden interactions due to limited shared resources (dCas9 and RBP-AD), which cause unexpected behavior. In contrast to the sequential reaction network observed for a single resource CRISPRa modality, the presence of two shared resources leads to a diamond-shaped reaction network responsible for two main outcomes. The first outcome is a self sequestration behavior, where an increase in the input after a certain threshold causes an unexpected decrease in the target protein concentration. The second outcome is the increased extent of off-target repression when compared to a single-resource CRISPRa (modality 1). In the future, we will explore the behavior of a network consisting of combined CRISPRa and CRISPRi systems. Furthermore, we will investigate control strategies to make CRISPRa robust to competition effects.

REFERENCES

[1] A. Koenig, "Competition for resources and its behavioral consequences among female primates," *International Journal of Primatology*, vol. 23, no. 4, pp. 759–783, 2002.

[2] A. L. Gulley, N. T. Nassar, and S. Xun, "China, the united states, and competition for resources that enable emerging technologies," *Proceedings of the national academy of sciences*, vol. 115, no. 16, pp. 4111–4115, 2018.

[3] G. M. Riegel, R. F. Miller, and W. C. Krueger, "Competition for resources between understory vegetation and overstory pinus ponderosa in northeastern oregon," *Ecological applications*, vol. 2, no. 1, pp. 71–85, 1992.

[4] X. Lambin, "Natal philopatry, competition for resources, and inbreeding avoidance in townsend's voles (microtus townsendii)," *Ecology*, vol. 75, no. 1, pp. 224–235, 1994.

[5] A. Gyorgy, J. I. Jiménez, J. Yazbek, H.-H. Huang, H. Chung, R. Weiss, and D. Del Vecchio, "Isocost lines describe the cellular economy of genetic circuits," *Biophysical journal*, vol. 109, no. 3, pp. 639–646, 2015.

[6] Y. Qian, H.-H. Huang, J. I. Jiménez, and D. Del Vecchio, "Resource competition shapes the response of genetic circuits," *ACS synthetic biology*, vol. 6, no. 7, pp. 1263–1272, 2017.

[7] P.-Y. Chen, Y. Qian, and D. Del Vecchio, "A model for resource competition in crispr-mediated gene repression," in *2018 IEEE Conference on Decision and Control (CDC)*. IEEE, 2018, pp. 4333–4338.

[8] H.-H. Huang, M. Bellato, Y. Qian, P. Cárdenas, L. Pasotti, P. Magni, and D. Del Vecchio, "dcas9 regulator to neutralize competition in crispri circuits," *Nature communications*, vol. 12, no. 1, pp. 1–7, 2021.

[9] S. Zhang and C. A. Voigt, "Engineered dcas9 with reduced toxicity in bacteria: implications for genetic circuit design," *Nucleic acids research*, vol. 46, no. 20, pp. 11 115–11 125, 2018.

[10] A. A. Dominguez, W. A. Lim, and L. S. Qi, "Beyond editing: repurposing crispr–cas9 for precision genome regulation and interrogation," *Nature reviews Molecular cell biology*, vol. 17, no. 1, pp. 5–15, 2016.

[11] M. Adli, "The crispr tool kit for genome editing and beyond," *Nature communications*, vol. 9, no. 1, pp. 1–13, 2018.

[12] J. G. Zalatan, M. E. Lee, R. Almeida, L. A. Gilbert, E. H. Whitehead, M. La Russa, J. C. Tsai, J. S. Weissman, J. E. Dueber, L. S. Qi *et al.*, "Engineering complex synthetic transcriptional programs with crispr rna scaffolds," *Cell*, vol. 160, no. 1-2, pp. 339–350, 2015.

[13] S. Clamons and R. Murray, "Modeling predicts that crispr-based activators, unlike crispr-based repressors, scale well with increasing grna competition and dcas9 bottlenecking," 2019.

[14] D. Del Vecchio and R. M. Murray, *Biomolecular feedback systems*. Princeton University Press, 2014.

[15] C. Dong, J. Fontana, A. Patel, J. M. Carothers, and J. G. Zalatan, "Synthetic crispr-cas gene activators for transcriptional reprogramming in bacteria," *Nature communications*, vol. 9, no. 1, pp. 1–11, 2018.